Electronic Supplementary Material (ESI) for ChemComm.

Supplementary Information

An efficient NiCu@C/Al_2O_3 catalyst for selective hydrogenation of acetylene

Shihong Zhou,[a] Chenyang Lu,*[a] Wenyu Zhou,[a] Yi Bi,[a] Cailong Zhou,[a] Aonan Zeng,[b] Anjie Wang,[b] Luxi Tan,[a] Lichun Dong*[a]

Table of Contents

1. Experiment section

1.1 Preparation of NiCu@C/Al_2O_3 catalysts

Firstly, stoichiometric $Cu(NO_3)_2 \cdot 3H_2O$ and $Ni(NO_3)_2 \cdot 6H_2O$ were dissolved in 200 mL deionized water to make a mixed solution. A certain amount of γ-Al_2O_3 was added to the above mixed solution under stirring for 5 h. After that, Na_2CO_3 solution was added to the mixture under vigorous stirring until pH = 10. After stirring for another 1 h, the obtained suspension was filtered and washed with deionized water to neutral. After drying for 12 h in vacuum oven, the solid was grounded to powder for further used as the catalyst precursor (denoted as NiCuCO_3^{2-}/Al_2O_3).

The obtained NiCuCO_3^{2-}/Al_2O_3 was treated in an acetylene-containing gas (10.0% C_2H_2 and 90.0% N_2) at 120℃ for 2 h with a heating rate of 3 ℃·min^{-1}. Then, the temperature was increased to 400 ℃ at a rate of 3 ℃·min^{-1} in the N_2 atmosphere for 1h. And then the gas was switched to H_2 for 3 h to obtain the Ni-Cu@C/Al_2O_3. For comparison, the NiCu/Al_2O_3 without carbon encapsulation was prepared without the treatment of the acetylene-containing gas.

1.2 Catalyst characterization

The crystal structure of catalysts was observed using an X-ray diffractometer (XRD) (PANalytical X'Pert Powder) with the CuKα radiation source (λ= 0.154 nm) at the scanning rate of 10 °·min^{-1} and the 2θ range is from 10° to 80°. Transmission electron microscopy (TEM), scanning transmission electron microscopy (STEM) and energy-dispersive X-ray spectroscopy (EDS) elemental mapping images were obtained on a Talos F200S microscope. X-ray photoelectron spectroscopy (XPS) characterization were obtained through a Scientific K-Alpha spectrometer with radiation of Al Kα (hv=1486.6 eV). The calibration peak is the C 1s peak at 284.8 eV. The images of morphology were taken on a Quattro S scanning electron microscope (SEM). The specific surface area

and the pore size distributions were calculated according to Bruner-Emmett-Teller (BET) method, and the physical adsorption and desorption of nitrogen at -196°C was measured by Micromeritics Tristar II 3020 instrument. The temperature programmed desorption of ammonia (NH_3-TPD) curves were obtained by Chembet-3000 instrument with a thermal conductivity detector (TCD) detector. Elemental analysis was carried out on a Vario EL Elemental analyzer. The thermal properties of catalysts in the flow of air were analyzed using a TG/DTA X70 thermogravimetric analyzer.

1.3 Catalytic Performance

The selective hydrogenation of acetylene was performed in a fixed-bed micro-reactor equipped with a 10 mm inner diameter quartz reaction tube which contained 0.1 g catalyst precursor and the catalysts were prepared *in situ* as described above. The reaction took place ranging from 80°C to 130°C with the feed gas (0.5% C_2H_2/ 10.0% H_2/ balance N_2) at a total flow rate of 30 mL·min^{-1} under the normal pressure. The gas composition before and after the reaction was analyzed by online gas chromatography (Nexis GC-2030) which was equipped with an FID detector and a capillary column (30 m × 0.535 mm×15.00 μm). Acetylene conversion and product selectivity were calculated as follows.

$$C_2H_2 \text{ conversion} = \frac{C_2H_2(\text{inlet}) - C_2H_2(\text{outlet})}{C_2H_2(\text{inlet})} \times 100\%$$

$$C_2H_6 \text{ selectivity} = \frac{C_2H_6(\text{outlet}) - C_2H_2(\text{inlet})}{C_2H_2(\text{inlet}) - C_2H_2(\text{outlet})} \times 100\%$$

$$C_2H_4 \text{ selectivity} = \frac{C_2H_4(\text{outlet}) - C_2H_4(\text{inlet})}{C_2H_2(\text{inlet}) - C_2H_2(\text{outlet})} \times 100\%$$

The selectivity of oligomer was determined by difference.

The acetylene hydrogenation in ethylene stream was performed over NiCu@C/Al_2O_3 with a mixture gas of 0.5% C_2H_2/ 10.0% H_2/ balance C_2H_4. And the selectivity to ethylene was obtained as : S(C_2H_4) = 1- S(C_2H_6)-S(C_4).

2. Figures

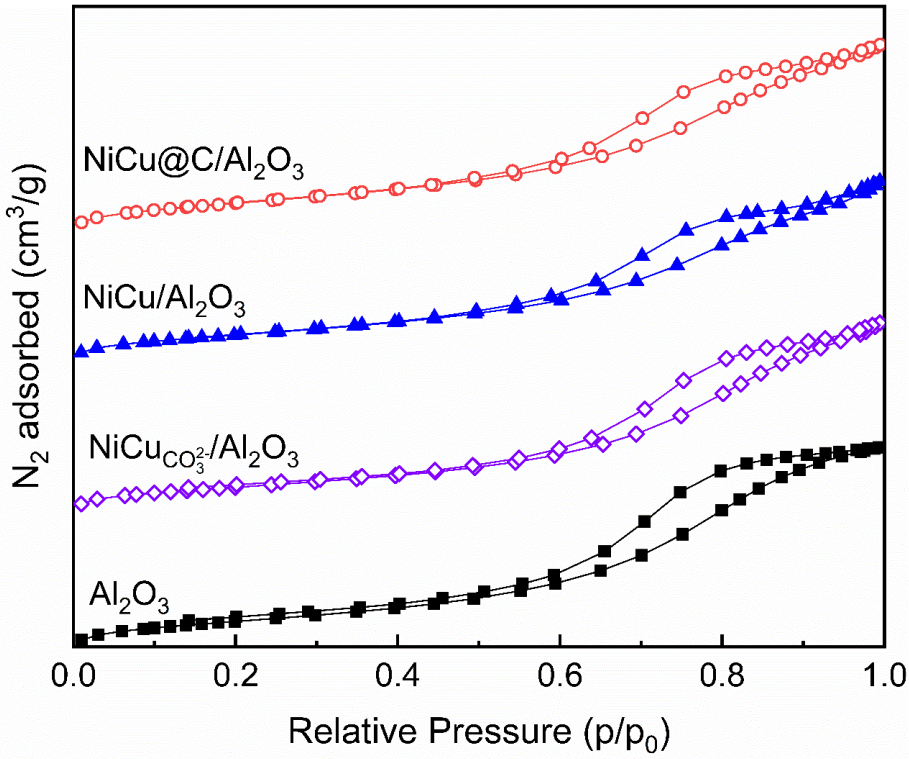

Fig. S1. N_2 adsorption-desorption isotherms of Al_2O_3, $NiCu_{CO_3^{2-}}/Al_2O_3$, $NiCu/Al_2O_3$ and $NiCu@C/Al_2O_3$.

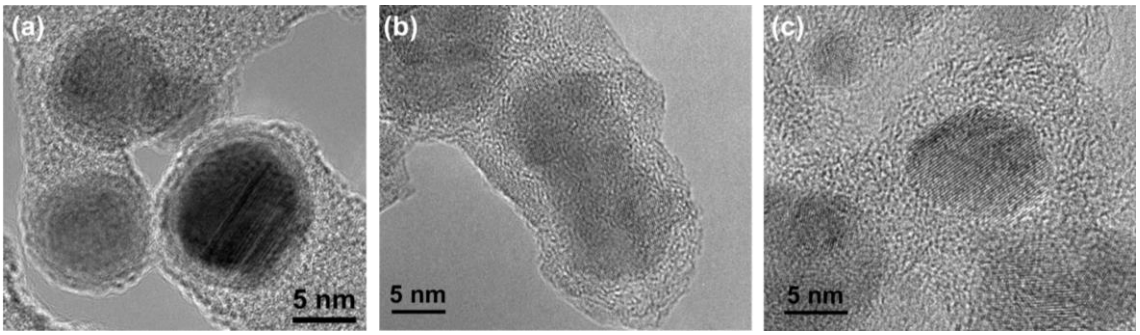

Fig. S2. TEM images of (a) $NiCu@C/Al_2O_3$, (b) $NiCu_2@C/Al_2O_3$ and (c) $Ni_3Cu_{10}@C/Al_2O_3$.

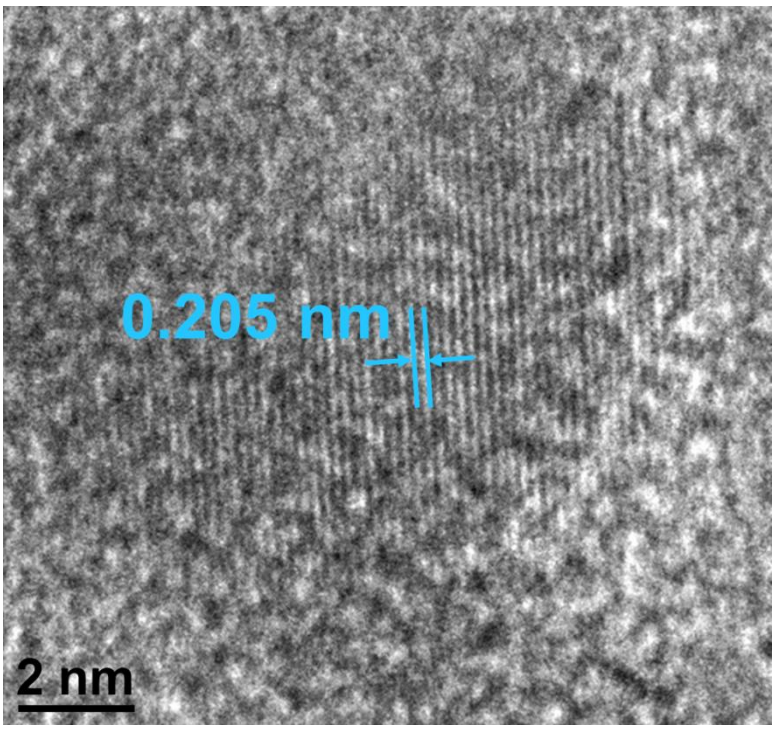

Fig. S3. HRTEM image of NiCu@C/Al_2O_3.

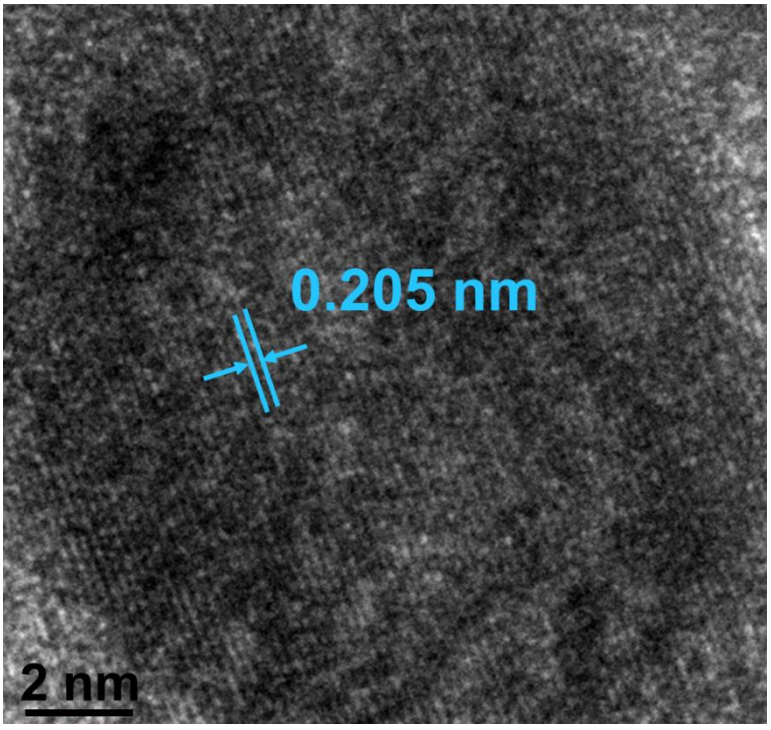

Fig. S4. HRTEM image of NiCu/Al_2O_3.

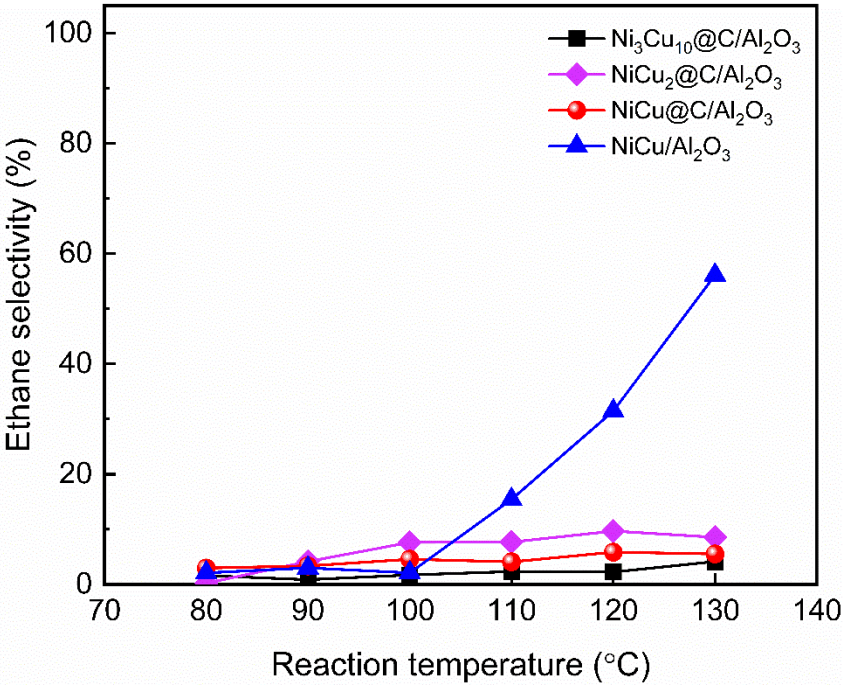

Fig. S5. Ethane selectivity of different catalysts as a function of reaction temperature.

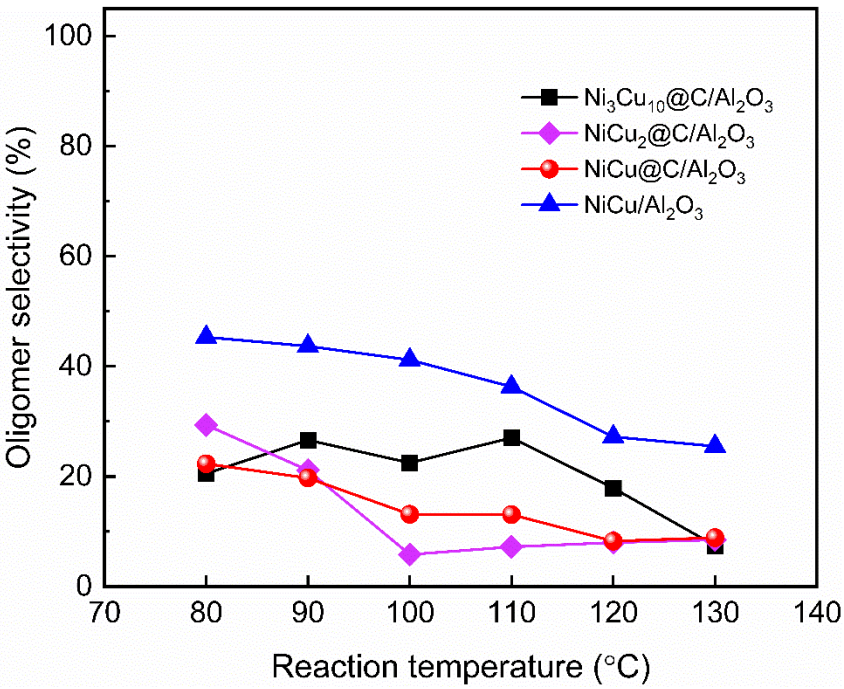

Fig. S6. Oligomer selectivity of different catalysts as a function of reaction temperature.

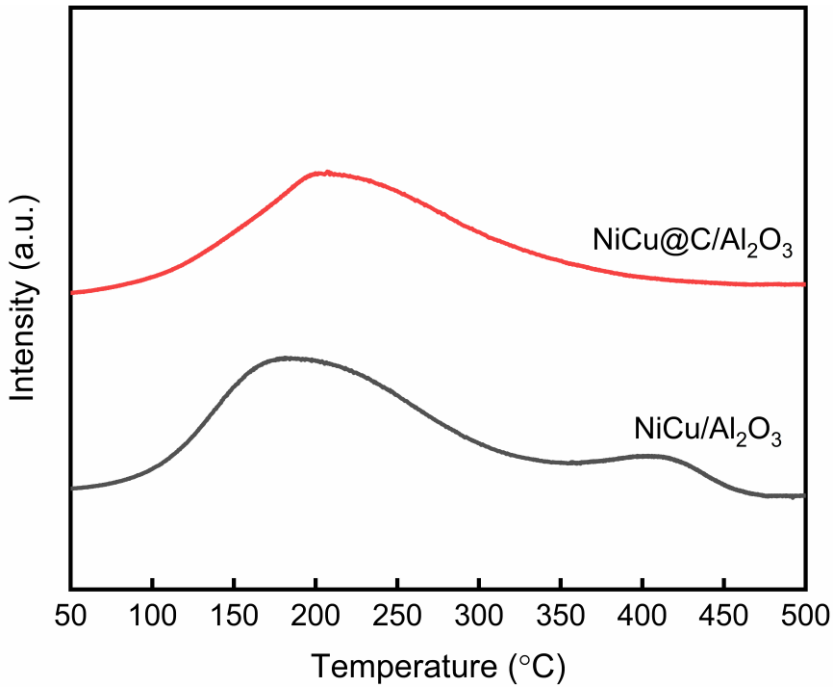

Fig. S7. NH_3-TPD curves of $NiCu@C/Al_2O_3$ and $NiCu/Al_2O_3$.

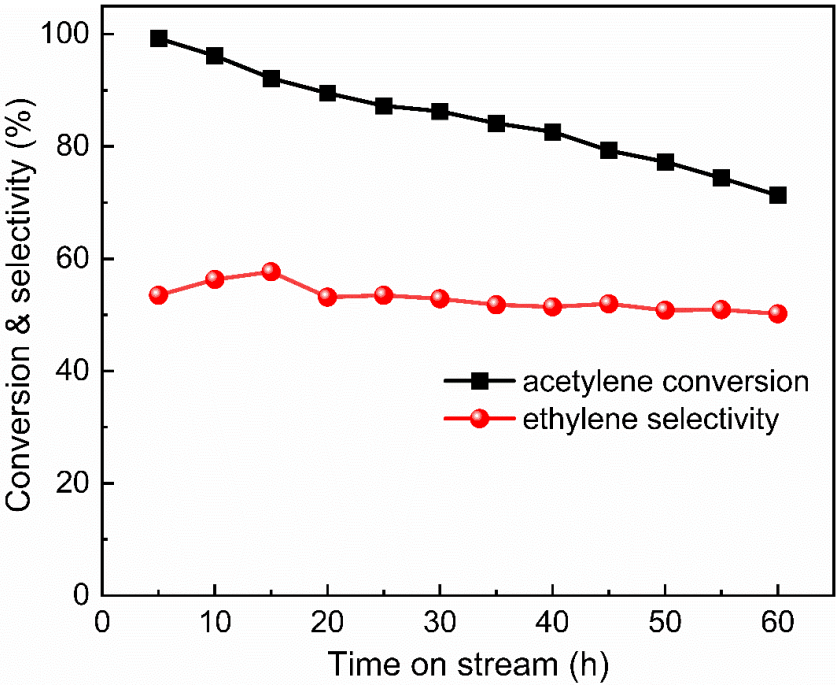

Fig. S8. Acetylene conversion and ethylene selectivity with time on stream over $NiCu@C/Al_2O_3$ at 90 °C.

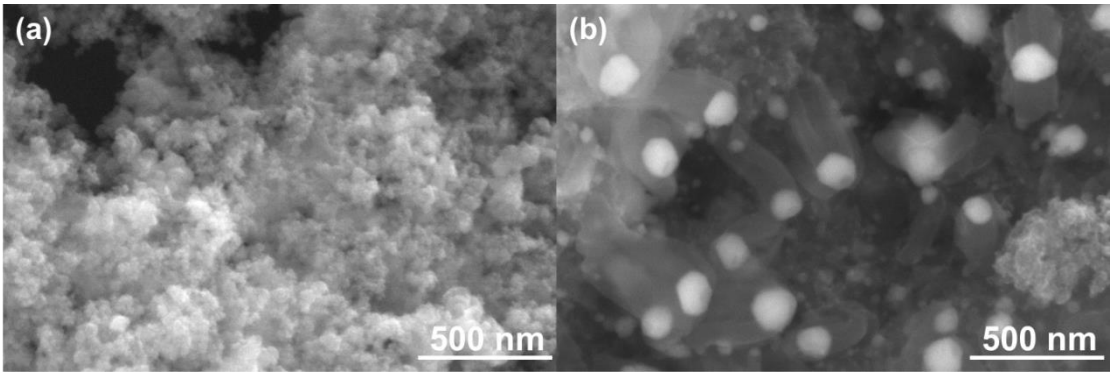

Fig. S9. SEM images of (a) NiCu@C/Al_2O_3 and (b) NiCu/Al_2O_3 after 40 h usage.

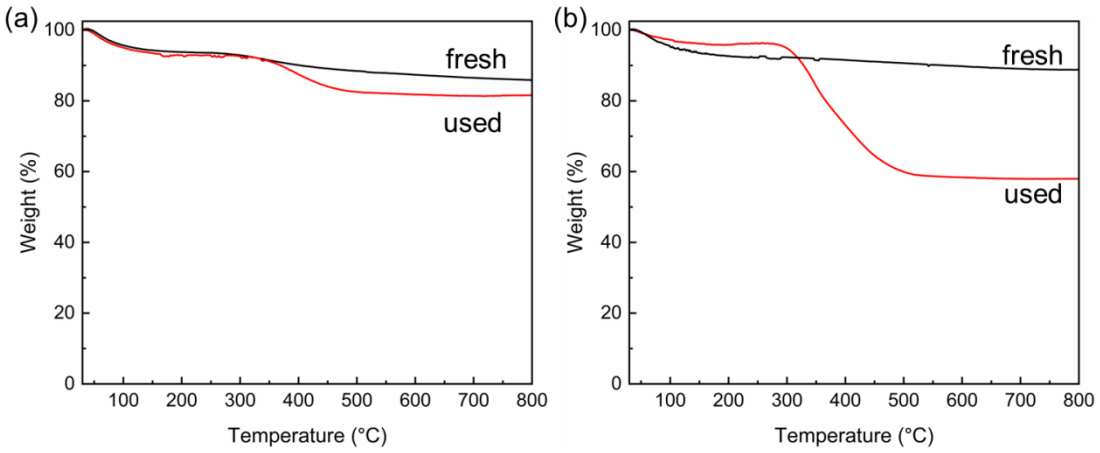

Fig. S10. TG curves of fresh and used (a) NiCu@C/Al_2O_3 and (b) NiCu/Al_2O_3 under air.

3. Tables

Table S1. Physical properties of Al_2O_3, $NiCu_{CO_3^{2-}}/Al_2O_3$, $NiCu/Al_2O_3$ and $NiCu@C/Al_2O_3$.

Catalysts	BET surface area (m^2/g)	Pore volume (cm^3/g)	Pore diameter (nm)
Al_2O_3	272	0.72	7.13
$NiCu_{CO_3^{2-}}/Al_2O_3$	233	0.64	7.84
$NiCu/Al_2O_3$	237	0.62	7.44
$NiCu@C/Al_2O_3$	269	0.65	7.22

Table S2. Elemental analysis of carbon.

Catalysts	$NiCu@C/Al_2O_3$	$NiCu_2@C/Al_2O_3$	$Ni_3Cu_{10}@C/Al_2O_3$
wt % carbon	1.1	1.6	3.1

Table S3. Comparison of catalytic performance over Ni-based catalysts.

Samples	T (℃)	Conversion (%)	Selectivity (%)	Reactants	Ref.
Ni-Cu@C/Al_2O_3	130	100	88	C_2H_2+H_2	This work
Ni-Cu@C/Al_2O_3	140	100	80	C_2H_2+H_2+C_2H_4	
NiCu/CeO_2	225	100	72.7	C_2H_2+C_2H_4	[1]
NiCu/MMO	160	100	70.2	C_2H_2+H_2+C_2H_4	[2]
Ni/MCM-41	250	100	47	C_2H_2+H_2	[3]
Ni/AC-N-0.5	200	96	46	C_2H_2+H_2	[4]
NiGa	260	100	82	C_2H_2+H_2	[5]
Ni_1Cu_2/g-C_3N_4	170	100	90	C_2H_2+H_2+C_2H_4	[6]
Na-Ni@CHA	180	100	97	C_2H_2+H_2	[7]
Ni-SAs/N-C	200	~95	90	C_2H_2+H_2+C_2H_4	[8]
Ni/SiO_2-Al_2O_3	175	8	60	C_2H_2+H_2	[9]
Ni/Al_2O_3	200	12	55	C_2H_2+H_2+C_2H_4	[10]
Ni_5Zn_{21}	160	75	50	C_2H_2+H_2+C_2H_4	[11]
NiZn/$MgAl_2O_4$	120	75	53	C_2H_2+H_2	[12]

References

[1] Y. Liu, A. J. McCue, P. Yang, Y. He, L. Zheng, X. Cao, Y. Man, J. Feng, J. A. Anderson, D. Li, *Chem. Sci.,* **2019**, *10*, 3556-3566.

[2] Y. Liu, J. Zhao, J. Feng, Y. He, Y. Du, D. Li, *J. Catal.,* **2018**, *359*, 251-260.

[3] S. Zhou, L. Kang, Z. Xu, M. Zhu, *RSC Adv.*, **2020**, *10*, 1937-1945.

[4] Z. Xu, S. Zhou, M. Zhu, *Catal. Commun.*, **2021**, *149*, 106241.

[5] Y. Cao, H. Zhang, S. Ji, Z. Sui, Z. Jiang, D. Wang, F. Zaera, X. Zhou, X. Duan, Y. Li, *Angew. Chem. Int. Ed.*, **2020**, *59*, 11647-11652.

[6] J. Gu, M. Jian, L. Huang, Z. Sun, A. Li, Y. Pan, J. Yang, W. Wen, W. Zhou, Y. Lin, H. J. Wang, X. Liu, L. Wang, X. Shi, X. Huang, L. Cao, S. Chen, X. Zheng, H. Pan, J. Zhu, S. Wei, W. X. Li, J. Lu, *Nat. Nanotechnol.*, **2021**, *16*, 1141-1149.

[7] Y. Chai, G. Wu, X. Liu, Y. Ren, W. Dai, C. Wang, Z. Xie, N. Guan, L. Li, *J. Am. Chem. Soc.*, **2019**, *141*, 9920-9927.

[8] X. Dai, Z. Chen, T. Yao, L. Zheng, Y. Lin, W. Liu, H. Ju, J. Zhu, X. Hong, S. Wei, Y. Wu, Y. Li, *Chem. Commun.*, **2017**, *53*, 11568-11571.

[9] C. Guimon, A. Auroux, E. Romero, A. Monzon, *Appl. Catal.*, *A*, **2003**, *251*, 199-214.

[10] S. Abelló, D. Verboekend, B. Bridier, J. Pérez-Ramírez, *J. Catal.*, **2008**, *259*, 85-95.

[11] C. S. Spanjers, J. T. Held, M. J. Jones, D. D. Stanley, R. S. Sim, M. J. Janik, R. M. Rioux, *J. Catal.*, **2014**, *316*, 164-173.

[12] D. L. Trimm, N. W. Cant, I. O. Y. Liu, *Catal. Today*, **2011**, *178*, 181-186.